Journal of Alloys and Compounds 520 (2012) 190–194

Contents lists available at SciVerse ScienceDirect

Journal of Alloys and Compounds

journal homepage: www.elsevier.com/locate/jallcom

Characterization of multiple metals (Cr, Mg) substituted $LiNi_{0.8}Co_{0.1}Mn_{0.1}O_2$ cathode materials for lithium ion battery

Bao Zhang[a], Lingjun Li[b], Junchao Zheng[a,*]

[a] School of Metallurgical Science and Engineering, Central South University, Changsha 410083, China
[b] School of Physics and Electronic Science, Changsha University of Science and Technology, Changsha 410114, China

ARTICLE INFO

Article history:
Received 2 November 2011
Received in revised form
30 December 2011
Accepted 2 January 2012
Available online 9 January 2012

Keywords:
Lithium ion battery
Cathode material
Cr
Mg
Substitution

ABSTRACT

Cr and Mg co-substituted $LiNi_{0.8}Co_{0.1}Mn_{0.1}O_2$ samples are synthesized by fast co-precipitation method and characterized by scanning electron microscope, X-ray diffraction, Rietveld refinement and electrochemical measurements. The Rietveld refinement results show that suitable Cr and Mg co-substitution could lead to synergistic reaction to form a kind of complementary structure, by full Cr occupying in Ni layer, and full Mg occupying in Li layer, respectively, and further attribute to highly ordered layered $LiNi_{0.8}Co_{0.1}Mn_{0.1}O_2$ with low cation mixing degree. Electrochemical studies demonstrate that Cr and Mg co-substitution in $LiNi_{0.8}Co_{0.1}Mn_{0.1}O_2$ also result in improved discharge capacity, initial coulombic efficiency, rate ability and cycling property compared to pristine $LiNi_{0.8}Co_{0.1}Mn_{0.1}O_2$. The improvements of electrochemical property resulted from the stabilized host structure by Cr and Mg incorporation into $LiNi_{0.8}Co_{0.1}Mn_{0.1}O_2$.

1. Introduction

Layered $LiNi_{0.8}Co_{0.1}Mn_{0.1}O_2$ have been intensively studied as a potential positive active electrode for application in plug-in hybrid electric vehicles (P-HEVs), due to its cheaper, higher capacity, and environmentally friendly characteristics compared with layered $LiCO_2$ [1–6]. However, its initial coulombic efficiency, rate capability and cycling performance are not satisfactory [7,8]. One possible reason is the similar radius of Ni^{2+} ion (0.69 Å) and Li^+ ion (0.76 Å) can cause cation mixing and then deteriorate the electrochemical performance of this material. Many authors reported that the substitution of Mg^{2+} ions, which are of a similar size to Li, in the lithium layer, can modify the structure of $Li(Ni_{1-x}M_x)O_2$ (M = metal) and improve the electrochemical performances [9–13]. So far, elements such as Cr have also been reported for partial substitution of Ni to improve discharge capacity and enhance the cycling performance of the cathode material, due to Cr^{3+} own electrochemical activity, and can reduce the cation mixing of $Li(Ni_{1-x}M_x)O_2$ (M = metal) [14–17]. From the above studies, it is noted that Cr or Mg substitution is conducive to improve structural stability of the cathode material, and Cr prefer to occupy transition metal site, Mg prefer to occupy Li site. However, studies about the effect of Cr and Mg co-substitution on $LiNi_{0.8}Co_{0.1}Mn_{0.1}O_2$ are less common. Woo et al. studied the impact of the Al and/or Mg substitutions on the $LiNi_{0.8}Co_{0.1}Mn_{0.1}O_2$ system and concluded that the improved structural stability and enhanced capacity of $Li[Ni_{0.8}Co_{0.1}Mn_{0.08}Al_{0.01}Mg_{0.01}]O_2$ is ascribed to Mg and Al co-substitution [9]. Thus, it is expected that a partial substitution of Cr and Mg would have positive effect to improve battery performances. In this work, we report effects of Cr and Mg co-substitution for $LiNi_{0.8}Co_{0.1}Mn_{0.1}O_2$ on structure and electrochemical property.

2. Experimental

2.1. Preparation of $LiNi_{0.8-x-y}Co_{0.1}Mn_{0.1}Cr_xMg_yO_2$

$LiNi_{0.8-x-y}Co_{0.1}Mn_{0.1}Cr_xMg_yO_2$ samples, labeled as (A) $x = y = 0$, (B) $x = 0.005$, $y = 0.015$, (C) $x = 0.01$, $y = 0.01$, and (D) $x = 0.015$, $y = 0.005$, were synthesized by fast co-precipitation and anneal method [18]: (1) $NiCl_2{\cdot}6H_2O$, $CoCl_2{\cdot}6H_2O$, $MnCl_2{\cdot}4H_2O$, $CrCl_3{\cdot}4H_2O$ and $MgCl_2{\cdot}6H_2O$ powders were dissolved in distilled water to obtain 2 mol/L solution. (2) The mixtures were filled in beaker and heated at 50 °C in water bath kettle, then $NH_3{\cdot}H_2O$ (2 M) and NaOH (2 M) were quickly poured into the solution to control the pH at 11.5. (3) After being reacted for 1 min under an Ar atmosphere, the mixtures were filtered, the resulting precursors were washed with distilled water and dried at 80 °C. (4) Finally, $LiOH{\cdot}H_2O$ was mixed with the precursors by hand force grinding for 0.5 h, and the obtained mixtures were sintered at 480 °C for 5 h, and then sintered at 750 °C for 15 h under O_2 atmosphere. An excess of lithium was used to compensate for lithium loss during the calcinations.

2.2. Sample characterization

The samples were analyzed by SEM (JEOL, JSM-5600LV). The powder X-ray diffraction (XRD, Rint-2000, Rigaku) using CuKα radiation was employed to identify

* Corresponding author. Tel.: +86 731 88836357.
E-mail addresses: tonyson.011@163.com, jczheng@csu.edu.cn (J. Zheng).

0925-8388/$ – see front matter © 2012 Elsevier B.V. All rights reserved.
doi:10.1016/j.jallcom.2012.01.004

Table 1
Results of the ICP analysis for $LiNi_{0.8-x-y}Co_{0.1}Mn_{0.1}Cr_xMg_yO_2$ samples: (A) $x=y=0$; (B) $x=0.005$, $y=0.015$; (C) $x=0.01$, $y=0.01$; (D) $x=0.015$, $y=0.005$.

Sample	Molar ratio of the final product (%)					
	Li	Ni	Co	Mn	Cr	Mg
A	1.000	0.802	0.099	0.099	0.000	0.000
B	1.008	0.778	0.094	0.098	0.006	0.016
C	1.003	0.781	0.097	0.097	0.011	0.011
D	0.995	0.782	0.100	0.103	0.014	0.006

the crystalline phase of the synthesized material. X-ray Rietveld refinement was performed by FULLPROF.

2.3. Electrochemical tests

The electrochemical properties of $LiNi_{0.8-x-y}Co_{0.1}Mn_{0.1}Cr_xMg_yO_2$ were measured by using 2025 button cell. Typical positive electrode loadings were in the range of 1.95–2 mg cm^{-2}, and an electrode diameter of 14 mm was used. The cathode consisted of 80 wt.% active material, 10 wt.% acetylene black and 10 wt.% PVDF binder. A lithium metal foil was used as anode. LiPF6 (1 M) in a 1:1:1 (v/v/v) mixture of dimethyl carbonate (DMC), Ethyl Methyl Carbonate (EMC) and ethylene carbonate (EC) was used as electrolyte. The assembly of the cells was carried out in a dry Ar-filled glove box. Electrochemical tests were carried out using an automatic galvanostatic charge–discharge unit, NEWARE battery cycler, between 2.7 and 4.3 V versus Li/Li$^+$ electrode at room temperature.

3. Results and discussion

The ICP results of $LiNi_{0.8-x-y}Co_{0.1}Mn_{0.1}Cr_xMg_yO_2$ (sample A, B, C and D) materials are reported in Table 1. It is noted that the chemical composition for each element in $LiNi_{0.8-x-y}Co_{0.1}Mn_{0.1}Cr_xMg_yO_2$ compounds is close to the stoichiometry. Fig. 1 exhibits typical XRD patterns of $LiNi_{0.8-x-y}Co_{0.1}Mn_{0.1}Cr_xMg_yO_2$ powders (sample A, B, C and D). All peaks are sharp and well-defined, suggesting that compounds are well crystallized. These diffraction peaks can be indexed on the basis of a hexagonal structure of α-$NaFeO_2$ (space group $R\bar{3}M$), and no impurity phase is detected in these patterns. It is believed that all elements are being incorporated within $LiNi_{0.8-x-y}Co_{0.1}Mn_{0.1}Cr_xMg_yO_2$ structure.

The lattice constants of the samples are shown in Table 2. It is observed that *a*, *c* lattice parameters and the unit cell volume decrease with Cr and Mg substitution, which is caused by slightly smaller ionic radius of Mg^{2+} (0.72 Å) and Cr^{3+} (0.615 Å) compared to that of Li^+ (0.76 Å) and Ni^{2+} (0.69 Å) [19], indicating that Mg is highly possible to occupy Li layer, and Cr is highly possible occupy

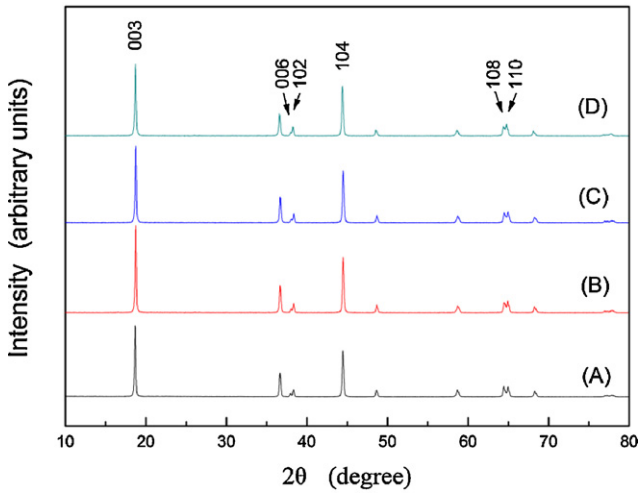

Fig. 1. XRD patterns of $LiNi_{0.8-x-y}Co_{0.1}Mn_{0.1}Cr_xMg_yO_2$ samples: (A) $x=y=0$; (B) $x=0.005$, $y=0.015$; (C) $x=0.01$, $y=0.01$; (D) $x=0.015$, $y=0.005$.

Table 2
Lattice parameters for $LiNi_{0.8-x-y}Co_{0.1}Mn_{0.1}Cr_xMg_yO_2$ samples: (A) $x=y=0$; (B) $x=0.005$, $y=0.015$; (C) $x=0.01$, $y=0.01$; (D) $x=0.015$, $y=0.005$.

Sample	*a* (Å)	*c* (Å)	$V_{hex.}$ (Å^3)	*c*/*a*
A	2.8720	14.1979	101.42	4.94356
B	2.8701	14.1920	101.24	4.94478
C	2.8680	14.1831	101.06	4.94530
D	2.8696	14.1863	101.15	4.94365

Ni layer. While *c*/*a* values exhibit hexagonal structure disorder are unchanged [20,21].

XRD patterns of all samples were further analyzed by Rietveld refinements, which were carried out assuming Li ions occupy the 3b site; Ni, Mn and Co are located in the 3a site, and O is located in the 6c site. In this work, we performed the refinements assuming several scenarios: full and partial occupation of Cr or Mg in the Li and/or Ni layers. For the samples C and D, with low Mg contents, the full occupation of Cr in Ni layer, and that of Mg in Li layer, results in the highest reliability factors. For the sample B, with high Mg contents, the partial occupation of Mg in both Li and Ni layer, and full occupation of Cr in Ni layer, results in the best reliability factors. As examples, the refinement results of samples B and

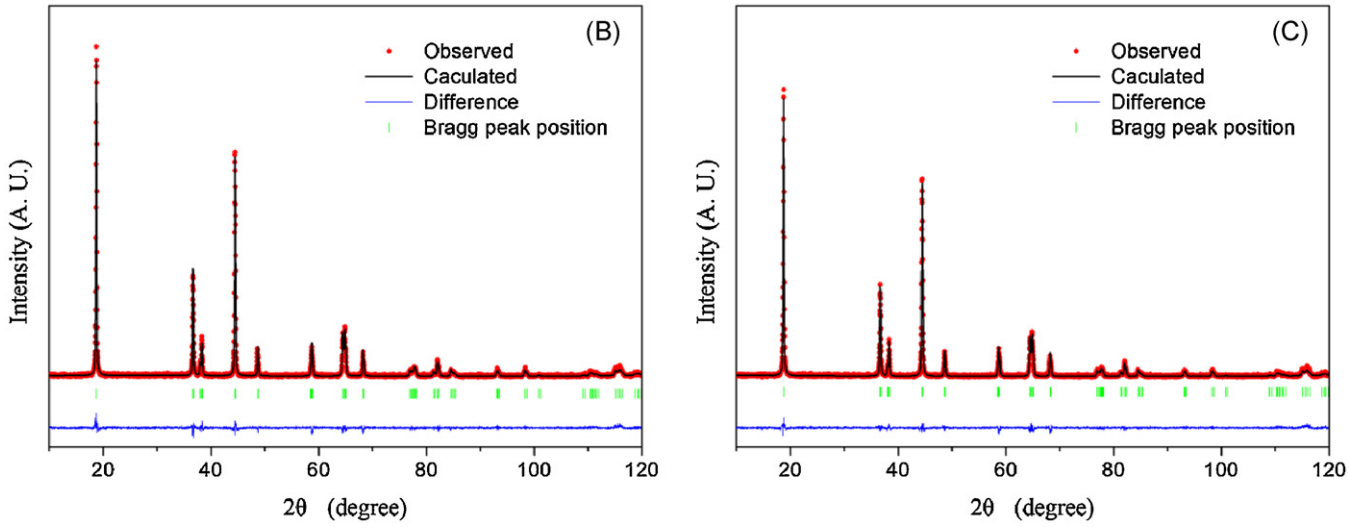

Fig. 2. Rietveld refinement results of X-ray diffraction patterns of $LiNi_{0.8-x-y}Co_{0.1}Mn_{0.1}Cr_xMg_yO_2$ samples: (B) $x=0.005$, $y=0.015$; (C) $x=0.01$, $y=0.01$.

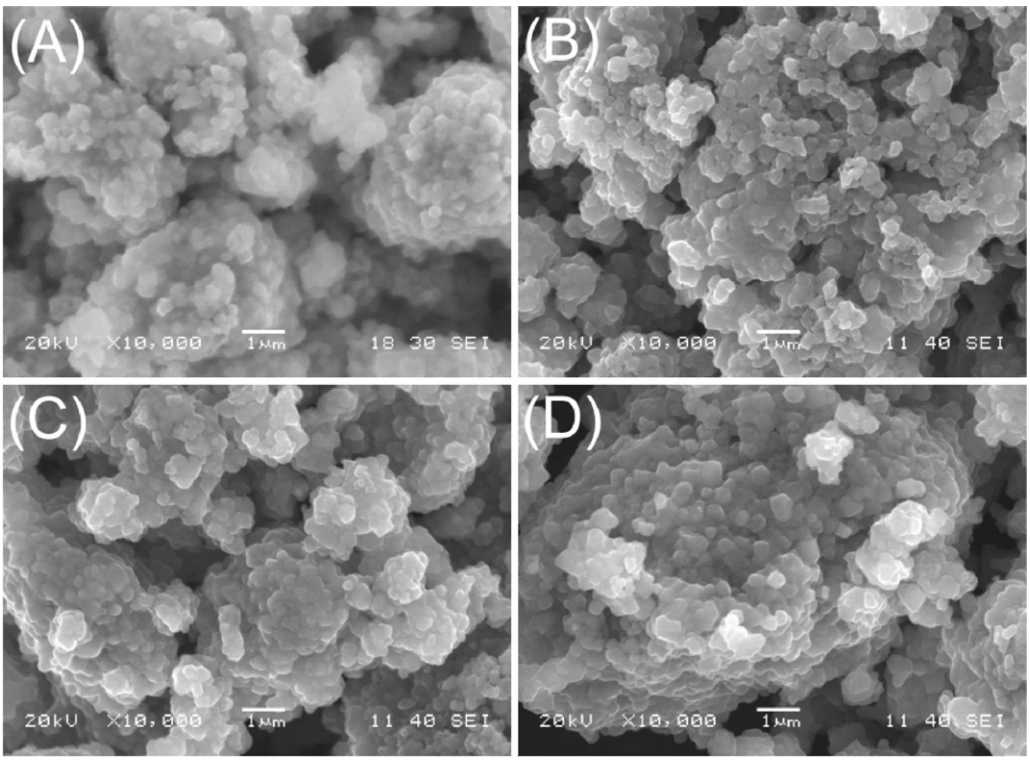

Fig. 3. SEM of $LiNi_{0.8-x-y}Co_{0.1}Mn_{0.1}Cr_xMg_yO_2$ samples: (A) $x = y = 0$; (B) $x = 0.005$, $y = 0.015$; (C) $x = 0.01$, $y = 0.01$; (D) $x = 0.015$, $y = 0.005$.

C are shown in Fig. 2. The good agreements between the calculated/experimental patterns demonstrate that these are successful refinements. The atom occupancies of all the samples are given in Table 3. It is noted that the Ni/Li mixing degree is reduced significantly by Cr and Mg substitution. It is also observed that, with Cr contents increasing from 0.005 (sample B) to 0.015 (sample D), and Mg contents decreasing from 0.015 (sample B) to 0.005 (sample D), the Ni/Li mixing degree reduces from 2.8 to 2.0, and then increases to 2.5, the sample C owns the best structure order.

The reason of structure improvement of Cr–Mg substituted $LiNi_{0.8}Co_{0.1}Mn_{0.1}O_2$ materials, especially the sample C, should be ascribed that suitable Cr and Mg co-substitution may lead to synergistic reaction to form a kind of complementary structure, by full Cr occupying in Ni layer, and full Mg occupying in Li layer, respectively, which could inhibit the Ni/Li mixing degree significantly. It is also noted that excessive Mg substitution could induce partial occupation of Mg in both Li and Ni layer (as shown in sample B), which might damage the structure of Ni layer, and weaken the effect of synergistic reaction between Cr and Mg substitution.

Table 3
Structural parameters obtained from Rietveld refinement of the XRD data for $LiNi_{0.8-x-y}Co_{0.1}Mn_{0.1}Cr_xMg_yO_2$ samples: (A) $x = y = 0$; (B) $x = 0.005$, $y = 0.015$; (C) $x = 0.01$, $y = 0.01$; (D) $x = 0.015$, $y = 0.005$.

Atom	Site	Occupancy			
		Sample A	Sample B	Sample C	Sample D
Li_1	3b	0.932 (4)	0.961 (2)	0.971 (4)	0.970 (3)
Mg_1	3b	0.000	0.011 (2)	0.009 (4)	0.005 (3)
Ni_2	3b	0.068 (4)	0.028 (2)	0.020 (4)	0.025 (3)
Ni_1	3a	0.802 (5)	0.800 (3)	0.796 (5)	0.782 (4)
Co_1	3a	0.099	0.094	0.097	0.100
Mn_1	3a	0.099	0.098	0.097	0.103
Cr_1	3a	0.000	0.004 (3)	0.010 (5)	0.015 (4)
Mg_2	3a	0.000	0.004 (3)	0.000 (5)	0.000 (4)
O	6c	2.000	2.000	2.000	2.000

Fig. 3 exhibits the SEM images of $LiNi_{0.8-x-y}Co_{0.1}Mn_{0.1}Cr_xMg_yO_2$ powders (sample A, B, C and D), which were sintered at 480 °C for 5 h, and then sintered at 750 °C for 15 h under O_2 atmosphere. As shown, there is no great difference between the particle size of sample A, B, C and D, which is about 100–400 nm, and all samples exhibit an uniform near-spherical microstructure. The agglomeration of $LiNi_{0.8-x-y}Co_{0.1}Mn_{0.1}Cr_xMg_yO_2$ powders (sample A and D) can be found from Fig. 3A and D, while there does not exist in $LiNi_{0.8-x-y}Co_{0.1}Mn_{0.1}Cr_xMg_yO_2$ powders (sample B and C) from Fig. 3B and C. From above it can come to a conclusion that the distribution of the $LiNi_{0.8-x-y}Co_{0.1}Mn_{0.1}Cr_xMg_yO_2$ powders is influenced by the introduction of Cr and Mg.

Fig. 4 shows the initial charge–discharge curves of the prepared $LiNi_{0.8-x-y}Co_{0.1}Mn_{0.1}Cr_xMg_yO_2$ powders (sample A, B, C and D),

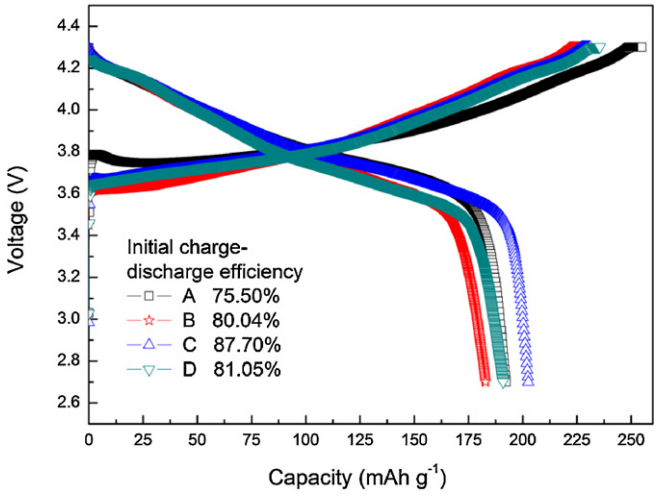

Fig. 4. Initial charge–discharge curves of $LiNi_{0.8-x-y}Co_{0.1}Mn_{0.1}Cr_xMg_yO_2$ samples: (A) $x = y = 0$; (B) $x = 0.005$, $y = 0.015$; (C) $x = 0.01$, $y = 0.01$; (D) $x = 0.015$, $y = 0.005$.

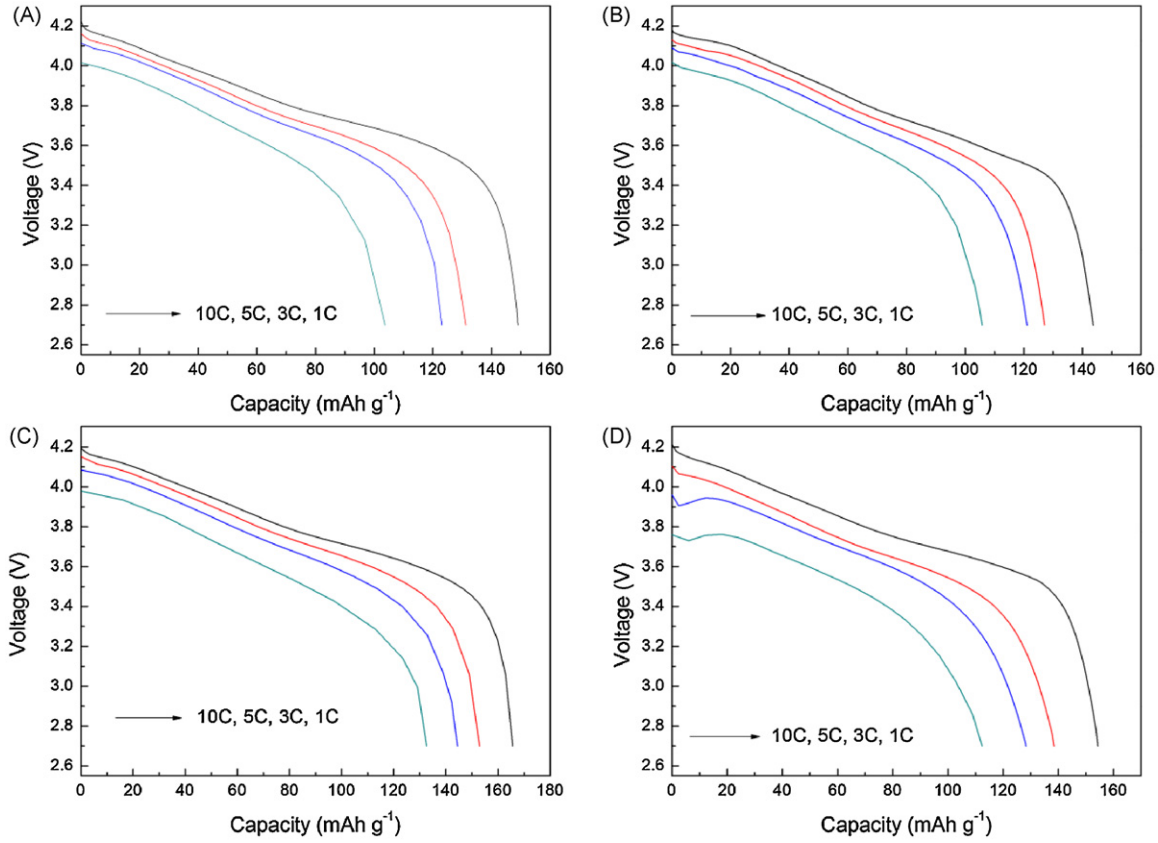

Fig. 5. Initial discharge curves of $LiNi_{0.8-x-y}Co_{0.1}Mn_{0.1}Cr_xMg_yO_2$ samples: (A) $x = y = 0$; (B) $x = 0.005$, $y = 0.015$; (C) $x = 0.01$, $y = 0.01$; (D) $x = 0.015$, $y = 0.005$, tested by various C-rates.

between 2.7 and 4.3 V under a current density of 18 mA g^{-1}. As shown in Fig. 4, the initial charge capacity of each sample (sample A, B, C and D) is 254.9 mAh g^{-1}, 228.4 mAh g^{-1}, 231.0 mAh g^{-1} and 235.55 mAh g^{-1}, respectively; the initial discharge capacity of each sample is 192.4 mAh g^{-1}, 182.8 mAh g^{-1}, 202.5 mAh g^{-1} and 190.9 mAh g^{-1}, respectively; and the initial charge–discharge efficiency of each sample is 75.5%, 80.04%, 87.7% and 81.05%, respectively.

It is noted that the initial charge and discharge capacity of the sample B is the lowest among all samples, which is due to the decrease in concentration of the active $Ni^{2+/3+}$ ions as the inactive Mg contents increases in the sample B [11]. While the coulombic efficiency of sample B is superior to that of sample A, this should be ascribed to Cr and Mg substitution decrease the Ni/Li mixing degree, as confirmed by Rietveld refinement. It is also observed that the initial discharge capacity and the coulombic efficiency of the sample C is the optimal. One of the reason is Cr substitution can increase the amount of electrochemical active component in compounds [14]. The other is related to the minimum cation mixing degree of the sample C, caused by synergistic reaction between suitable Cr and Mg substitution.

Fig. 5 presents the rate capability of the prepared $LiNi_{0.8-x-y}Co_{0.1}Mn_{0.1}Cr_xMg_yO_2$ powders (sample A, B, C and D). The cells were charged to 4.3 V at 0.1, 1, 3 and 5 C, and then discharged to 2.7 V at 1, 3, 5 and 10 C, respectively. Although the discharge capacity of sample A is higher than that of the sample B at 1 C, it drops off dramatically with increasing C-rates. The discharge capacities of sample A are from 148.9 mAh g^{-1} at 1 C to 131.3 mAh g^{-1}, 123.1 mAh g^{-1} and 103.7 mAh g^{-1} at 3, 5 and 10 C, which are only 78.2%, 68.2%, 63.9% and 53.9% of the discharge capacity at 0.1 C. However, the rate capability is improved dramatically by Cr and Mg substitution. The sample B presents discharge capacity of 143.6 mAh g^{-1}, 127.1 mAh g^{-1}, 121.1 mAh g^{-1} and 105.81 mAh g^{-1} at 1, 3, 5 and 10 C, corresponding to 78.5%, 69.5%, 66.2% and 57.9% of its capacity of 182.8 mAh g^{-1} at 0.1 C. The sample C, with the minimum cation mixing degree, shows the discharge capacity of 165.7 mAh g^{-1}, 152.9 mAh g^{-1}, 144.4 mAh g^{-1} and 132.6 mAh g^{-1} at 1, 3, 5 and 10 C, corresponding to 81.8%, 75.5%, 71.3% and 65.5% of its capacity of 202.5 mAh g^{-1} at 0.1 C. Hence, Cr and Mg substitution is favorable to improve the rate capability of $LiNi_{0.8}Co_{0.1}Mn_{0.1}O_2$.

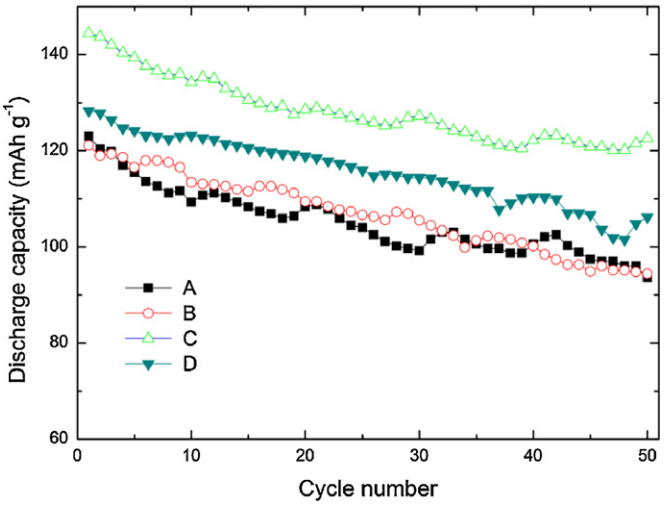

Fig. 6. Cycling performance of $LiNi_{0.8-x-y}Co_{0.1}Mn_{0.1}Cr_xMg_yO_2$ samples: (A) $x = y = 0$; (B) $x = 0.005$, $y = 0.015$; (C) $x = 0.01$, $y = 0.01$; (D) $x = 0.015$, $y = 0.005$, tested at 5 C.

The cycling stability of $LiNi_{0.8-x-y}Co_{0.1}Mn_{0.1}Cr_xMg_yO_2$ powders (sample A, B, C and D) is given in Fig. 6. The cells were initially charged at 3 C, and then discharged and charged at 5 C in the range of 2.7–4.3 V for 50 times. The wavy curves should be ascribed to room temperature change. The retained discharge capacity for each sample after 50 cycles is 93.6 mAh g^{-1}, 94.45 mAh g^{-1}, 122.5 mAh g^{-1} and 106.18 mAh g^{-1}, respectively, which is 76.1%, 78.0%, 84.8% and 82.7% of its initial discharge capacity, respectively. It is obvious that the long-term cyclic performance is improved by Cr and Mg substitution, and the sample C has the highest discharge capacity and best cycling performance. This is consistent with the Rietveld refinement results. The high discharge capacity and stable cycling performance of the $LiNi_{0.78}Co_{0.1}Mn_{0.1}Cr_{0.01}Mg_{0.01}O_2$ could attribute to its well-defined structure.

4. Conclusion

Cr and Mg co-substituted $LiNi_{0.8-x-y}Co_{0.1}Mn_{0.1}Cr_xMg_yO_2$ powders were successfully synthesized by fast co-precipitation method. XRD analysis found that all elements are being incorporated within $LiNi_{0.8-x-y}Co_{0.1}Mn_{0.1}Cr_xMg_yO_2$ powders structure, and no impurity phase is detected in these patterns. Rietveld refinements shown that suitable Cr and Mg co-substitution could lead to synergistic reaction to form a kind of complementary structure, by full Cr occupying in Ni layer, and full Mg occupying in Li layer, respectively, and further attribute to highly ordered layered $LiNi_{0.8}Co_{0.1}Mn_{0.1}O_2$ with low cation mixing degree. Electrochemical studies confirm that the $LiNi_{0.78}Co_{0.1}Mn_{0.1}Cr_{0.01}Mg_{0.01}O_2$ exhibits the highest discharge capacity of 202.5 mAh g^{-1}, 165.7 mAh g^{-1}, 152.9 mAh g^{-1}, 144.4 mAh g^{-1} and 132.6 mAh g^{-1} at 0.1, 1, 3, 5 and 10 C, and the capacity retention after 50 cycles at 5 C is 84.8%. It is concluded that the reduced cation mixing and improved structure stability are due to the enhancement of rate characteristic and cyclability caused by Cr and Mg substitution.

Acknowledgments

This study was supported by National Natural Science Foundation of China (Grant No. 51072233), the Freedom Explore Program of Central South University (No. 2011QNZT070), Planned Science and Technology Project of Hunan Province, China (Grant No. 2010FJ6024), and Postdoctoral Sustentation Fund of Central South University, China.

References

[1] M.-H. Kim, H.-S. Shin, D. Shin, Y.-K. Sun, J. Power Sources 159 (2006) 1328–1333.
[2] Y.K. Sun, S.T. Myung, B.C. Park, J. Prakash, I. Belharouak, K. Amine, Nat. Mater. 8 (2009) 320–324.
[3] J. Eom, M.G. Kim, J. Cho, J. Electrochem. Soc. 155 (2008) A239–A245.
[4] J.J. Saavedra-Arias, N.K. Karan, D.K. Pradhan, A. Kumar, S. Nieto, R. Thomas, R.S. Katiyar, J. Power Sources 183 (2008) 761–765.
[5] L. Croguennec, Y. Shao-Horn, A. Gloter, C. Colliex, M. Guilmard, F. Fauth, C. Delmas, Chem. Mater. 21 (2009) 1051–1059.
[6] Y.X. Gu, F.F. Jian, J. Phys. Chem. C 112 (2008) 20176–20180.
[7] Y.K. Sun, S.T. Myung, M.H. Kim, J.H. Kim, Electrochem. Solid-State Lett. 9 (2006) A171–A174.
[8] J. Cho, T.J. Kim, J. Kim, M. Noh, B. Park, J. Electrochem. Soc. 151 (2004) A1899–A1904.
[9] S.W. Woo, S.T. Myung, H. Bang, D.W. Kim, Y.K. Sun, Electrochim. Acta 54 (2009) 3851–3856.
[10] C. Pouillerie, L. Croguennec, C. Delmas, Solid State Ionics 132 (2000) 15–29.
[11] J. Cho, Chem. Mater. 12 (2000) 3089–3094.
[12] W.B. Luo, F. Zhou, X.M. Zhao, Z.H. Lu, X.H. Li, J.R. Dahn, Chem. Mater. 22 (2010) 1164–1172.
[13] W.B. Luo, X.H. Li, J.R. Dahn, J. Electrochem. Soc. 157 (2010) A993–A1001.
[14] Y.C. Sun, Y.G. Xia, H. Noguchi, J. Power Sources 159 (2006) 1377–1382.
[15] N.K. Karan, M. Balasubramanian, D.P. Abraham, M.M. Furczon, D.K. Pradhan, J.J. Saavedra-Arias, R. Thomas, R.S. Katiyar, J. Power Sources 187 (2009) 586–590.
[16] L.J. Li, X.H. Li, Z.X. Wang, H.J. Guo, P. Yue, W. Chen, L. Wu, J. Alloy Compd. 507 (2010) 172–177.
[17] A. Sakunthala, M.V. Reddy, S. Selvasekarapandian, B.V.R. Chowdari, P. Christopher Selvin, Electrochim. Acta 55 (2010) 4441–4450.
[18] L.J. Li, X.H. Li, Z.X. Wang, H.J. Guo, P. Yue, W. Chen, L. Wu, Powder Technol. 206 (2011) 353–357.
[19] R. Shannon, Acta Crystallogr. 32 (1976) 751–767.
[20] T. Ohzuku, A. Ueda, M. Nagayama, J. Electrochem. Soc. 140 (1993) 1862–1870.
[21] X.M. Wang, X.Y. Wang, S.Y. Yi, J.Q. Cao, Chin. J. Process Eng. 7 (2007) 817–821.